SWDC-4 LARGE FORMAT DIGITAL AERIAL CAMERA SYSTEM

Jian Li[a, b,*], Xianlin Liu[b], Fengde Liu[b],Zongjie Liu[b] Liping Zhao[b]

[a]School of Information Engineering in Remote Sensing, Wuhan University， 129 Luoyu Road, Wuhan 430079,China - lijian_bj@sina.com

[b]Chinese Academy of Surveying and Mapping,16 Beitaiping Road, Beijing 100039,China - lijian_bj@sina.com

Commission III, WG III/3

KEY WORDS: Digital Aerial Camera, Calibration, Accuracy, Analysis

ABSTRACT:

Digital aerial imaging becomes a hot topic since the ISPRS congress 2000 in Amsterdam. Now, there are approximately 120 high-end or "large format" systems available. However, the price of those cameras is high, and most of them have problems such as a large number of image pairs to handle and lower height accuracy as compared with traditional aerial cameras. Siwei Digital Camera-4 (SWDC-4) is a large format aerial camera developed by Beijing Geo-Vision Tech.Co.,Ltd. in 2006 for meeting the need of topographical mapping. SWDC-4 is composed of four non-metric unit cameras or camera heads. It is of following main characteristics: changeable lens, large field-of-view (71^o/92^o), large base-to-height ratio (0.58/0.82 at 60% overlap), and high height accuracy. The paper describes the SWDC-4 large format digital aerial camera system in details. After a brief description of the system constellation special attention is paid to some key techniques, i.e. (a) calibration of non-metric CCD cameras, (b) correction and rectification of unit images (c) internal bundle adjustment, (d) generation of virtual image. The results of the test block in Beijing are presented. The relative height accuracy of both GPS-supported aerial triangulation and absolute orientation for single pair can reach 1/10000. The geometric accuracy of stereo mapping from the view of convergent photography is analysed in details. The high geometric accuracy achieved by SWDC-4 is mainly backdated to its large field-of-view and large base-to-height ratio, and the reliable measurability based on the high quality of digital image. The experimental result proved that SWDC-4 meets the accuracy request of stereo mapping.

1. INTRODUCTION

Advantages of digital cameras are widely understood: No film, no photo lab, no scanning, no noise from film grain and no cost of duplication (Leberl et al., 2002). Superior radiometry promises more flying days and easier interpretation, also more success of automated procedures (Leberl et al., 2003). Highly abundant image data can be obtained, so as that in the post-processing, multiple-baseline stereo method can be used to get the high-density point clouds. According to (Heipke et al., 2006), frame based as well as linear array cameras are available on the market and, although exact numbers are difficult to specify, approximately 120 high-end or "large format" systems (Leica ADS40, Intergraph DMC, Vexcel Ultra-Cam-D). But the price of those cameras is high, and most of them have the problems such as a large number of image pairs to handle and lower height accuracy as compared with traditional aerial cameras (cf. Zhang, 2004).

Siwei Digital Camera-4 (SWDC-4) is a large format aerial camera developed by Beijing Geo-Vision Technologies Co., Ltd. in 2006 for meeting the need of topographical mapping. SWDC-4 is composed of four non-metric unit cameras or camera heads. It is of following main characteristics: changeable lens, large field-of-view (71^o/92^o), large base-to-height ratio (0.58/0.82 at 60% overlap), and high height accuracy.

After a brief description of the system constellation special attention is paid to some key techniques, i.e. (a) calibration of non-metric CCD cameras, (b) correction and rectification of unit images (c) internal bundle adjustment, (d) generation of virtual image. Results of the test block in Beijing are presented. The relative height accuracy of both GPS-supported aerial triangulation and absolute orientation for single image pair can reach 1/10000. The geometric accuracy of stereo mapping from the view of convergent photography is analysed in details. The high geometric accuracy achieved by SWDC-4 is mainly backdated to its large field-of-view and large base-to-height ratio, and the reliable measurability based on the high quality of digital image. The experimental result proved that SWDC-4 meets the accuracy request of stereo mapping.

2. SYSTEM

SWDC-4 (Fig. 1) consists of among others following system components:

- four Hasselblad H1D unit cameras or heads, which build up the main camera body,
- a PCl04 computer, which is responsible for communications between different system components and their controls,
- a stabilised platform, which serves to stabilise the camera during image acquisition ,
- a L1/L2 GPS receiver, whose data is used for the aircraft guidance and image exposure control during the flight and

* Corresponding author. Lijian_bj@sina.com, Tel: 86-10-68221079

for the GPS-supported aerial triangulation in the post processing ,

- an automatic synchronous exposure control system with fixed point,
- a digital compass for automatic drift correction.

Fig.1 SWDC－4 digital camera

The key problem of the camera is the synchronization of exposures of individual heads. Differences in exposure time could lead to an instable relative geometry of projection centers of images taken by individual unit heads (e.g. ca. 12cm at aircraft speed of 150km/h). The instable geometry makes the virtual image generation much more difficult than expected as designed. Fig. 2 shows the principle of automatic synchronous exposure control with fixed point. PC104 receives GPS coordinates from the GPS receiver in 5Hz and compares them with the ones of exposure points planned. Once a planned point is reached, exposure signal is sent to the automatic synchronous exposure control system and the time is then recorded. After exposure, the signals of individual heads return to the PC104 respectively, and the signal of head 4 (as reference head) will simultaneously be sent to the GPS receiver for recording as exposure mark of the camera. More than one thousand experiments with SWDC-4 were conducted and found out that the time difference between individual heads is less than 3 ms, which can be compensated very well in the later virtual image generation (cf. 3.3 below).

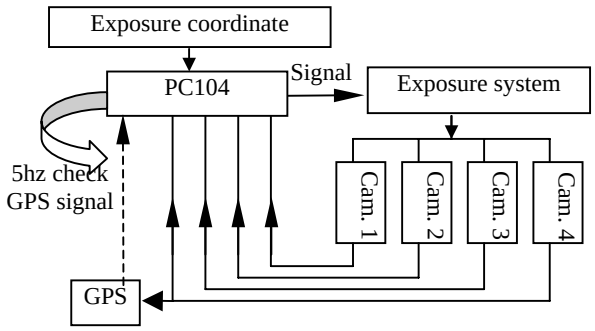

Fig. 2 SWDC-4 control of exposure synchronously

3. GENERATOIN OF VIRTUAL IMAGE

Since large format CCD is hardly available yet for technological and economical reasons, techniques of combining small-sized CCD cameras to make a large format camera are adopted, and thus a large format so-called virtual image can be computed from individual small-sized images (Tang et al., 2000). As shown in Fig. 3, using the conjugate points in the overlap area of unit images captured by individual heads, an internal bundle adjustment is executed to accurately compute the parameters of relative orientation between them. Based on the computed parameters, the unit images are then projected to a virtual image plane respectively. In general, the approach mainly consists of four processing steps: (a) calibration of non-metric CCD camera, (b) correction and rectification of unit images (c) internal bundle adjustment, (d) generation of virtual image.

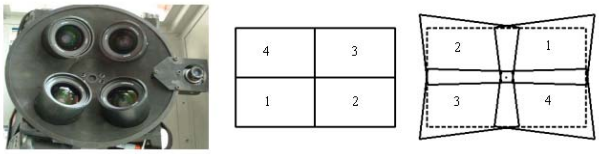

Fig.3 Camera heads and origin, rectified Image

3.1 Camera calibration

Calibration of a camera is to determine its elements of interior orientation and lens distortion (Wang, 1990). It is prerequisite of photogrammetric processing and an important factor of quality improvement. Different from other cameras, the unit cameras used here are non-metric cameras that have instable elements of interior orientation and large lens distortions. Thus high precision calibration must be carried out for each unit camera firstly. After taking pictures of a control field with hundreds high precision targets, we use the software Australis (Fraser, 1997) for a separate bundle adjustment to calculate the following parameters: elements of interior orientation (f,x_0,y_0),radial lens distortion (K_1,K_2,K_3), decentering distortion (P_1 P_2), in-plane distortion (b_1,b_2). The accuracy of elements of interior orientation amounts to better than 1μm, and meets the accuracy request of stereo mapping in practice.

3.2 Correction and rectification

Using the calibrated parameters each unit image can be corrected to an ideal image with the principal point at (0, 0) and without lens distortions according to the following formula (1) (cf. Fraser, 1997):

$$\begin{aligned}\Delta x &= \bar{x}r^2K_1+\bar{x}r^4K_2+\bar{x}r^6K+(2\bar{x}+r^2)P_1+2P_2\bar{x}\bar{y}+b_1\bar{x}+b_2\bar{y}_3\\ \Delta y &= \bar{y}r^2K_1+\bar{y}r^4K_2+\bar{y}r^6K+2P_1\bar{x}\bar{y}+(2\bar{y}+r^2)P_2\end{aligned} \quad (1)$$

where $\bar{x}=x-x_0, \bar{y}=y-y_0, r=\sqrt{\bar{x}^2+\bar{y}^2}$,

(x, y) are the coordinates of the image point. Fig.5-b is an example of the corrected image. To check the quality of the calibration and correction, we re-calibrate the camera using the corrected images, so that the principal point of each unit head tends to be at (0,0) and distortion parameters become tenth or even hundredth of the ones before.

Image rectification is the process of transforming the obliquely obtained image (ideal image or corrected image) into a horizontal equivalent image (rectified image e.g. Fig.5-c) of the

same scale based on projective geometry. The relationship between point "a" in oblique image and point "a^0" in horizontal equivalent image is shown as Fig. 4.

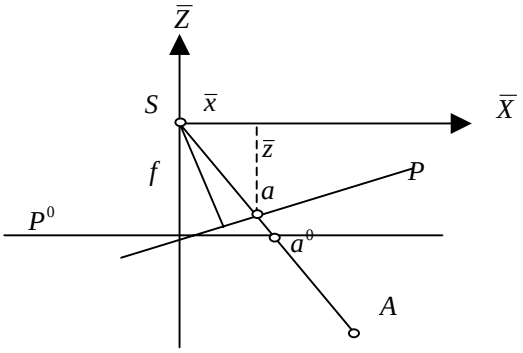

Fig.4 Principle of image rectification

The purposes of correction and rectification are that it can provide more convenience for image matching and generation of virtual image.

3.3 Internal bundle adjustment

In the overlap area (cf. Fig. 3), matching homologous points is a pre-condition for the generation of virtual image, also must be fast, stable and high in precision. Harris corner detector (Harris and Stephens, 1988) is a popular interest point detector due to its strong invariance to (Schmid et al., 2000): rotation, scale, illumination variation and image noise. The harris corner detector is based on the local auto-correlation function of a signal, where the local auto-correlation function measures the local changes of the signal with patches shifted by a small amount in different directions. It has the advantages of simplicity and stability. So we use harris corner detector to extract feature points. Then, a pseudo matching set with pixel precision is obtained by comparing local neighbourhoods of features through intensity cross-correlation method and least squares matching (LSM)(Ackermann, 1984) is used to get pseudo matching set with (high) sub-pixel precision. These pseudo matches are divided into inliers and outliers using robust RANSAC algorithm (Fischler et al., 1981), thus most gross error will be eliminated, the remains will be picked out in the processing of internal bundle adjustment.

Internal bundle adjustment is the core of sub-image mosaic. It computes the parameters of relative orientation between the individual rectification images with a high precision. Different from the traditional bundle adjustment, internal bundle adjustment involves a displacement due to the slightly different location of the projection center of unit camera (Madani, 2004). Internal bundle adjustment is rational under a horizontal reference plane on which has not terrain relief. In practice, it is impossible. But further researches indicate the error （systematic displacement）could be neglected in a certain surroundings(Tang et al., 2000).

Assuming the projection center of unit image 1 is at the origin of a local coordinate system, i.e. its elements of exterior orientation are all zero, and the elements of exterior orientation of other three individual unit images are $\{Dx_i, Dy_i, Dz_i, \varphi_i, \omega_i, \kappa_i\}(i = 2 \sim 4)$. Although the error of synchronous exposure can be kept less than 3ms, Dx_i, Dy_i, (i=2~4) are still inconstant. We use GrafNav/Net software to calculate the exact values based on GPS exposure mark and time differences. Dz_i (i=2~4) can be observed as zero. The rotation matrices are of:

$$R_i = \begin{bmatrix} a_{i1} & a_{i2} & a_{i3} \\ b_{i1} & b_{i2} & b_{i3} \\ c_{i1} & c_{i2} & c_{i3} \end{bmatrix}$$

$$a_{i1} = \cos\varphi_i \cos\kappa_i - \sin\varphi_i \sin\omega_i \sin\kappa_i$$
$$a_{i2} = -\cos\varphi_i \sin\kappa_i - \sin\varphi_i \sin\omega_i \cos\kappa_i$$
$$a_{i3} = -\sin\varphi_i \cos\omega_i$$
$$b_{i1} = \cos\varphi_i \sin\kappa_i$$
$$b_{i2} = \cos\omega_i \cos\kappa_i$$
$$b_{i3} = -\sin\omega_i$$
$$c_{i1} = \sin\varphi_i \cos\kappa_i + \cos\varphi_i \sin\omega_i \sin\kappa_i$$
$$c_{i2} = -\sin\varphi_i \sin\kappa_i + \cos\varphi_i \sin\omega_i \cos\kappa$$
$$c_{i3} = \cos\varphi_i \cos\omega_i$$

Therefore, considering the influence of Dx and Dy only, the coordinates (x_i', y_i') after rotation and transformation of point (x_i, y_i) in rectified image from unit camera 2-4 can be calculated by the formula:

$$\begin{aligned} x_i' &= -f\frac{a_{i1}x_i + a_{i2}y_i - a_{i3}f}{c_{i1}x_i + c_{i2}y_i - c_{i3}f} + kDx_i \\ y_i' &= -f\frac{b_{i1}x_i + b_{i2}y_i - b_{i3}f}{c_{i1}x_i + c_{i2}y_i - c_{i3}f} + kDy_i \end{aligned} \quad (2)$$

where $k = \frac{f}{H}$, H is average flying height above the ground. i=2~4. Theoretically homologous points should have the same coordinates in the virtual image, i.e.:

$$\begin{aligned} x_i' - x_j' &= 0 \\ y_i' - y_j' &= 0 \end{aligned} \quad (3)$$

where i and j have four groups of value: (i，j)={(1，2)，(1，4)，(2，3)，(3，4)}, and $x_1' = x_1, y_1' = y_1$； Now we can get eight equations including $\varphi_i, \omega_i, \kappa_i (i = 2,3,4)$ 9 parameters (or unknowns). However there are residuals of those equations in practice, substituting（2）into（3）and linearizing them yields the following error equations (4):

$$\begin{aligned} v_{xij} &= -f(1+\frac{x^2}{f^2})\Delta\varphi_i - \frac{xy}{f}\Delta\omega_i + y\Delta\kappa_i + f(1+\frac{x^2}{f^2})\Delta\varphi_j - \frac{xy}{f}\Delta\omega_j - y\Delta\kappa_j - l_x \\ v_{yij} &= \frac{xy}{f}\Delta\varphi_i - f(1+\frac{y^2}{f^2})\Delta\omega_i - x\Delta\kappa_i + \frac{xy}{f}\Delta\varphi_j + f(1+\frac{y^2}{f^2})\Delta\omega_j + x\Delta\kappa_j - l_y \end{aligned} \quad (4)$$

where $l_x = x_i'^0 - x_j'^0; l_y = y_i'^0 - y_j'^0$.

(a) Original images

(b) Corrected images

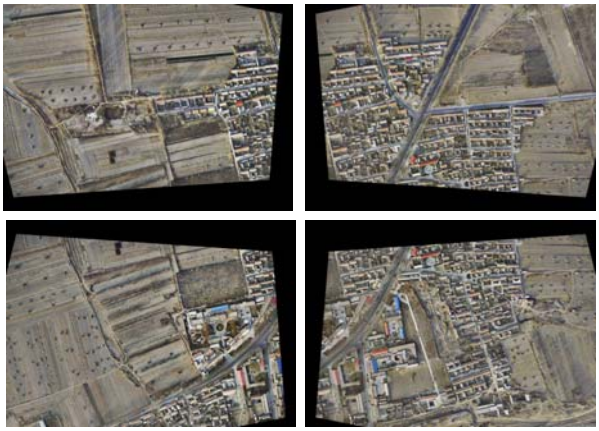

(c) Rectified images

(d) Virtual image

Fig. 5 Generation of virtual image

Based on these error equations, normal equations can be formed through conventional methods. The solution of the normal equations would give the corrections of the parameters. Since the coefficients are taken from the first derivative term of Taylor's formula and the approximation values of parameters are usually coarse, the method of successive approximation should be applied in computation. In each approximation, if the maximum residual of point is more than three times of mean square error, this point is considered a gross error and is eliminated. The final value of a parameter is the sum of its initial value and corrections obtained in the approximations.

3.4 Mosaiking of image

Based on the computed parameters from section 3.3, the unit images are projected to a virtual image plane respectively. Virtual projection center is the projection center of unit head 1. Thus, projecting the unit images of 2-4 to the virtual image plane (i.e. unit image 1) using formula (2), the virtual image can be produced. Fig.5-d is an example of virtual image.

4. RESULTS

On December 2006 image data of the Beijing BaDaLing block are taken at a flight altitude of 550m above ground level, which corresponds to a ground sampling distance (GSD) of 10cm. Camera parameters are 9μm pixel size, 50mm focal length and 11500×8000 resolution. The block (Fig. 6) covers a rectangular of 7km×2.5km and consists of 178 images distributed in 6 parallel strips. The forward overlap is 80 percent and side overlap is 60 percent. Baseline length is 200m.The block contains 58 full GCP that is used as check points and orientations. The area of high-density GCP has 30 points and is used to test the results of accuracy of absolute orientation for single pair. The results from JX4-C DPW system are demonstrated in table 1. Table 1 shows that the precision is proportional to the overlap, that is, the influence related to the virtual image generation due to offset in projection center and terrain relief is small and negligible.

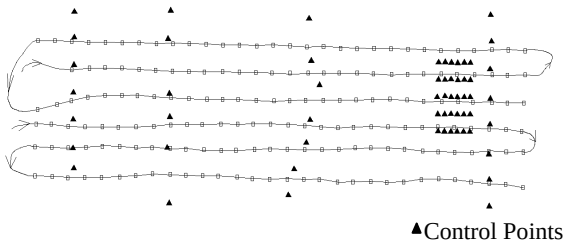

Fig.6 Control Points Distribution of BaDaLing Block

Pairs	RMS X	RMSY	RMSX Y	RMS Z	Num.	overlap
84－85	5.5	3.3	6.4	8.1	23	81%
84－86	4.0	4.1	5.7	5.5	23	63%
84－87	2.6	2.8	3.8	4.3	23	49%
85－87	4.8	3.7	3.7	6.1	23	63%
24－26	4.4	3.6	5.6	5.7	20	63%
25－27	3.1	4.0	5.0	5.9	24	63%

Tab.1 Accuracy of Absolute Orientation for Single Pair (unit: cm)

The GPS-supported aerial triangulation is done using Geoload-AT, PATB, DPGrid, WuCAPS software respectively to prove the stability of virtual images. The results are listed in table 2. The relative height accuracy of GPS-supported aerial triangulation with more than 40 check points can reach 1/10000, and is better than analog camera's. And the result is much better than the requirements of aerial photographic specification. It shows that the SWDC mosaic model and design are stable and reliable.

Softare package	Orientation points					Check points						Note
	RMS X	RMS Y	RMS Z	No. of horizontal point	No. of vertical point	RMS X	RMS Y	RMS Z	No. of horizontal point	No. of vertical point	Height relative precision	
Geoload-AT	3.4	4.0	5.7	15	15	6.8	7.0	4.9	42	42	1/11327	60%,60%,1
Geoload-AT	6.5	7.5	5.9	11	11	8.1	7.5	7.3	39	39	1/7600	60%,30%,1
PATB	5.0	2.0	1.1	4	4	6.1	7.0	7.4	48	48	1/7500	60%,60%,2
PATB	0.3	0.4	0.2	4	4	4.2	5.9	5.4	48	48	1/10278	80%,60%,2
DPGrid	6.3	3.8	7.2	4	4	4.0	10.4	7.5	48	48	1/7400	60% 60%,2
DPGrid	1.9	2.7	3.5	4	4	2.9	4.7	5.0	48	48	1/11100	80%,60%,2
WuCAPS	-	-	-	4	12	5.0	7.0	5.5	44	36	1/10090	60%,30%,1
WuCAPS	-	-	-	4	15	7.0	4.0	6.2	48	37	1/8952	80%,60%,1

Note：The values in last column mean forward overlap, side overlap and configuration of orientation points, which "1" and "2" denote respectively 4-XYZ ground control points around the corners of block area and two rows of vertical ground control points near the ends of block are used in GPS-supported bundle block adjustment.

Tab.2 Results of GPS-supported aerial triangulation (unit：cm)

5. ACCURACY ANALYSES OF STEREO MAPPING

We got a good results mentioned above using SWDC-4 camera in practice. This chapter analyses the geometric error and accuracy of stereo mapping from the view of convergent photography in detail. Since the high-resolution image is assembled from 4 views taken with oblique unit heads, each covering a quarter of the virtual image, the essence of stereo mapping is the convergent photography of oblique cameras.

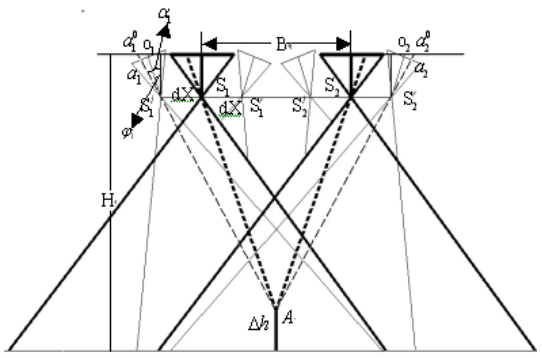

Fig.7 SWDC stereo model

Fig. 7 shows a stereo pair of SWDC-4 image. B is the baseline; φ_1, φ_2 are the photographic convergent angle; The virtual image planes is drawn in bold line and unit image planes is on the left and right sides. The coordinates of one object A can be calculated by both normal photography of virtual image and convergent photography of individual unit image with a systematic error. Now we discuss the accuracy of A point in convergent photography. It can be approximately estimated through equivalent normal case photography.

The formula on the accuracy of object point coordinates in normal photography is (Feng, 2002):

$$M_Z = k_1 k_2 \sqrt{m_{x_1}^2 + m_{x_2}^2} \tag{5}$$

where, $k_1 = \frac{H}{B}$, $k_2 = \frac{H}{f}$, H and B is average flight height and baseline length respectively, m_{x_1}, m_{x_2} are the accuracy of the image point coordinates.

Assuming $\varphi = \varphi_1, \alpha = \alpha_1$, the equations between point a_1^0 （$\bar{x}, \bar{y}$）in the equivalent normal case photography and point a_1 （x, y）in convergent photography are :

$$\left.\begin{aligned} \bar{x} &= \frac{f(x\cos\varphi + f\sin\varphi)}{f\cos\varphi - x\sin\varphi} \\ \bar{y} &= \frac{f}{f\cos\varphi - x\sin\varphi} \end{aligned}\right\} \tag{6}$$

After derivation, the corrections from convergent photography to equivalent normal case photography are:

$$\left.\begin{aligned} d_{\bar{x}} &= \frac{1 + \tan\alpha \tan\varphi}{1 - \tan(\alpha - \varphi)\tan\varphi} d_x \\ d_{\bar{y}} &= \frac{\sec\varphi}{1 - \tan(\alpha - \varphi)\tan\varphi} d_y \end{aligned}\right\} \quad (7)$$

where, d_x and d_y are the errors of the image point coordinates in convergent photography.

The corrections due to the displacement in projection center are (Tang et al., 2000)：

$$\left.\begin{aligned} \Delta_x &= \frac{f}{H - \Delta h} \frac{\Delta h / H}{H(1 - \Delta h / H)} dX_0 \\ \Delta_y &= \frac{f}{H - \Delta h} \frac{\Delta h / H}{H(1 - \Delta h / H)} dY_0 \end{aligned}\right\} \quad (8)$$

Summing up the (7) and (8), we get the coordinate offset in the virtual image plane:

$$\left.\begin{aligned} d_{x_v} &= d_{\bar{x}} + \Delta_x \\ d_{y_v} &= d_{\bar{y}} + \Delta_y \end{aligned}\right\} \quad (9)$$

Substituting equation (7) and (8) into (9) and applying the law of error propagation, we get:

$$\left.\begin{aligned} m_{x_v} &= \sqrt{d_{\bar{x}}^2 + \Delta_x^2} = \sqrt{\left(\frac{1 + \tan\alpha\tan\varphi}{1 - \tan(\alpha - \varphi)\tan\varphi} m_x\right)^2 + \Delta_x^2} \\ m_{y_v} &= \sqrt{d_{\bar{y}}^2 + \Delta_y^2} = \sqrt{\left(\frac{1 + \tan\alpha\tan\varphi}{1 - \tan(\alpha - \varphi)\tan\varphi} m_x\right)^2 + \Delta_y^2} \end{aligned}\right\} \quad (10)$$

Only considering height accuracy, substituting equation (10) into (5), we obtain the accuracy equation (11):

$$M_Z = k_1 k_2 \sqrt{\left(\frac{1+\tan\alpha_1\tan\varphi}{1-\tan(\alpha_1-\varphi)\tan\varphi}\right)^2 m_{x_1}^2 + \left(\frac{1+\tan\alpha_2\tan\varphi}{1-\tan(\alpha_2-\varphi)\tan\varphi}\right)^2 m_{x_2}^2 + 2\Delta_x^2} \quad (11)$$

The equation indicates that the accuracy in height of SWDC-4 virtual image is mainly related to the parameters k_1 (namely baseline-to-height ratio), m_x (the accuracy of the image point coordinates) and Δ_x. The base-to-height ratio (0.58/0.82 at 60% overlap) of SWDC-4 is equal or greater than the ratio (0.58) of RC30 and is approximately two times of DMC's(0.31). This is one of the most important reasons that SWDC-4 has high height accuracy. The accuracy of the image point coordinates is usually 1/3 pixel size in analog images, but investigations (Alamús et al., 2006) indicate that the accuracy improves by a factor of 1.3 comparing manual point identification in digital images to analog images, thus the value of m_x is about 1/4 pixel (i.e. 2.5μm). In our test mentioned above, f=50mm,H=550m, $\Delta h = 50m$, B=400m(60% overlap), $\varphi = 20^\circ$, substituting those values to equation (11), we obtain the accuracy value in theory, as illustrated by the curve (middle) in Fig. 4(X-axis means the plane distance from current point to left projection center in the direction of base line). The results between 5.6cm and 5.9 cm are coherent to the results in Fig. 1.The influences of offset in projection center and terrain relief are also shown in Fig.4 in different values of Δh. According to equation (8), the error due to the displacement in projection center is 0.22cm when $\Delta h / H$ equals to 0.1, and is just 1.0cm under 0.2.

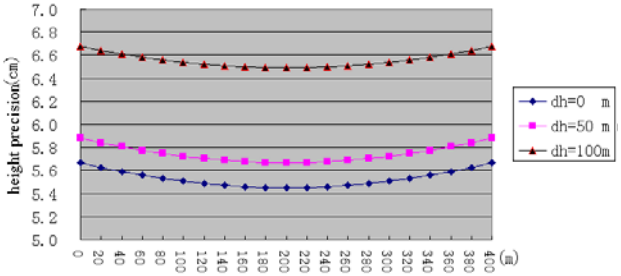

Fig.4 Influence of topographic relief on the height accuracy

6. CONCLUSIONS

The results on the test block of Beijing show that the relative height accuracy of GPS-supported aerial triangulation and absolute orientation for single pair can reach 1/10000 respectively, is higher than the analog and some digital cameras because of large base-to-height ratio and high quality images. Analyses of the geometric error and accuracy of stereo mapping in theory show that the results in practice are fully consistent in the results in theory and the influence related to the virtual image generation due to offset in project center and terrain relief is small and negligible. All things have proved the feasibility and reliability of mosaic model and rationality of design and SWDC-4 can meets the accuracy request of mapping, especial the medium and small-scale topography maps in national fundamental surveying and mapping. The SWDC-4 has wide prospect of application and popularisation.

ACKNOWLEDGEMENTS

We gratefully thank Dr. Tang Lang for guidance and suggestions of the paper.

REFERENCES

Ackermann, F. (1984). High Precision Digital Image Correlation. Proceedings of the 39th. Photogrammetric Week, 19-24, Sept., Stuttgart, Germany, pp. 231-243

Alamús R., Kornus W., Talaya J.. (2006), Studies on DMC geometry. ISPRS Journal of Photogrammetry & Remote Sensing 60 (2006) 375–386.

Harris C. and Stephens M.J. (1988). A combined corner and edge detector. In Alvey Vision Conference, pages 147–152,)

Heipke, C., Jacobsen, K., Mills, J. (2006). Editorial of Theme issue: "Digital aerial cameras" ISPRS Journal of Photogrammetry & Remote Sensing 60 (2006) 361–362

Feng Wen Hao.(2002) Close-range Photogrammetry. Wuhan: WuHan University press,2002 ,pp 63-67

Fischler M A, Bolles R C. (1981) Random sample consensus: a Paradigm for model fitting with application to image analysis and automated cartography [J]. CommunicationAssociation Machine, ,24(6):381～395.]

Fraser, C.S. (1997). Digital camera self-calibration. ISPRS Journal of Photogrammetry and Remote Sensing 52 (4), 149–159.

Leberl, F. et al. (2003): The UltraCam Large Format Aerial Digital Camera System, Proceedings of the American Society For Photogrammetry & Remote Sensing, 5-9 May, 2003, Anchorage,Alaska

Leberl F., R. Perko, M. Gruber, M. (2002) Ponticelli.Novel Concepts for Aerial Digital Cameras.Symposium of ISPRS-Commission I, Denver(Colorado). ISPRS-Archives, Volume 34, Part 1.Available from GITC bv., Lemmer, The Netherlands.)

Madani, M., Dörstel C., Heipke C., Jacobsen K. (2004): DMC practical experience and accuracyassessment. In: ISPRS Proceedings 2004 Istanbul.

Schmid C., Mohr R., and Bauckhage C.. (2000). Evaluation of interest point detectors.International Journal of Computer Vision, 37(2):151–172, June

Tang, L., Dörstel, C., Jacobsen, K., Heipke, C., Hinz, A. (2000). Geometric accuracy potential of the digital modular camera. International Archives of Photogrammetry and Remote Sensing33, 1051–1057 (Part B4/3).

Wang Zhi Zhuo.(1990) Principles of Photogrammetry. Wuhan: Press of WTUSM,1990,pp 168-169

Zhang Zu Xun.(2004). Aspects on aerial digital cameras. Engineering of Surveying and Mapping Vol.13,No.5.